
New angles in motional averaging

A. Samoson, B. Q. Sun, and A. Pines

It is the dispersion of local magnetic fields—the spread of resonant frequencies inherent even in the simplest systems—that determines selectivity and resolution in NMR. The local fields among a group of coupled nuclei, for example, may be rendered non-stationary owing to spin flip-flops, or spin diffusion, and the associated resonance can acquire a certain width as a result. Another source of frequency dispersion arises from the dependence of most spin interactions on the orientation of the external magnetic field relative to each nucleus. Thus both the spin and spatial dependence of the magnetic interactions must be addressed if one is to realize full spectroscopic control in NMR.

Local fields are manifested in different ways in solids and liquids, and spectroscopic methods need to be tailored accordingly. At one extreme there is the case of an isotropic liquid where, in the presence of rapid and random molecular reorientation, spatial anisotropy is averaged largely to zero. For sufficiently rapid tumbling, only the isotropic components of the spin interactions remain and so it becomes possible to achieve truly high resolution. In solids, however, restrictions on molecular motion prevent the spins from sampling a spherically symmetric set of orientations. Here, there are two general solutions: either remove the field altogether, and by so doing eliminate the very notion of directionality, as in zero-field NMR (this eliminates also the distinct isotropic chemical shifts of different nuclei), or, alternatively, one can impose an artificial motion on the spins to create the equivalent of a spherically symmetric environment. This latter option, that of supplying the motion externally, was inherent in the spin echo experiment [1] and its generalizations [2] in which the spin angular momenta are perturbed while leaving the molecules in place; and in the sample-spinning experiments of Anderson [3], in which the sample is rotated. Averaging in spin space has progressed from simple spin echoes to the prolonged trains introduced by Waugh and later workers for solids [4]. Averaging in real space was extended to solids by magic angle spinning (MAS) [5,6] which, today, is a routine feature of solid state NMR. In this chapter we consider some new approaches that extend motional averaging in solid state NMR, with particular emphasis on the NMR of systems governed by electric quadrupole interactions.

In designing suitable averaging techniques, one should realize first that it is unnecessary to implement full spherical symmetry. Since the anisotropy of the

spin interactions is well defined and limited, only a subset of the full rotation group is needed for efficient averaging. The problem then becomes one of determining what trajectories are both adequate and also feasible to implement through bulk macroscopic motions.

The orientational dependence of a nuclear or electronic dipolar transition frequency can be represented formally as a sum of components, each irreducible under the rotation group $SO(3)$:

$$\omega = \sum_l \omega_l \quad (3.1)$$

The contribution of each component ω_l depends on the $2l+1$ values of the corresponding tensor A_{lm} , which forms the basis of the representation $D^{(l)}$ of $SO(3)$. It also depends on the orientation $\Omega^{\text{SFC}} = (\alpha, \beta, \gamma)$ of the magnetic field in a sample-fixed coordinate (SFC) system (Fig. 3.1); namely

$$\omega_l = \sum_m A_{lm} D_{m0}^{(l)}(\Omega^{\text{SFC}}), \quad (3.2)$$

where $D_{m0}^{(l)}$ is an element of the associated Wigner rotation matrix (which is also a representation of the full rotation group). The particles in a heterogeneous

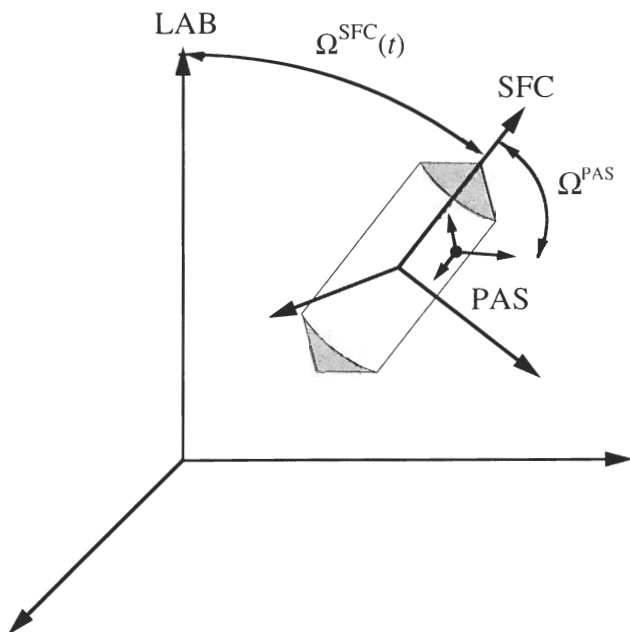


Fig. 3.1 Two successive sets of Euler angles determine the direction of the magnetic field relative to the sample-fixed coordinates (SFC) and the principle axis system (PAS) at each nuclear site.

sample are randomly oriented, and hence exhibit different sets of values A_{lm} :

$$A_{lm} = \sum_n \rho_{ln} D_{nm}^{(l)}(\Omega^{\text{PAS}}), \quad (3.3)$$

where the ρ_{lm} denote principle tensor components of rank l . Dispersion in the Euler angles Ω^{PAS} , reflecting different orientations of the sample-fixed coordinate frame relative to the local principal axis system (PAS), is the formal reason behind inhomogeneous line broadening (or modulation of the intensity in optical spectroscopy or NQR). The isotropic part of the frequency in eqn (3.1), ω_0 , is the same for each particle in the sample and thus is potentially measurable with the highest analytical resolution.

Spectroscopic measurement always requires a finite time to establish the differences between energy levels, during which the system continues to evolve and during which one can change the relative direction of the fields and of the sample. The orientation of the SFC, in general, is a function of time, and its motion impresses a time dependence upon the transition frequency. The observed phase of the signal, at some instant T , is proportional to

$$\phi_l(T) = \int_0^T dt \omega_l(t) = \sum_m A_{lm} \int_0^T dt D_{m0}^{(l)}\{\Omega^{\text{SFC}}(t)\}, \quad (3.4)$$

which reflects the cumulative effects of the changing resonant frequency assuming no geometric phase is accumulated [7]. Stroboscopic measurement

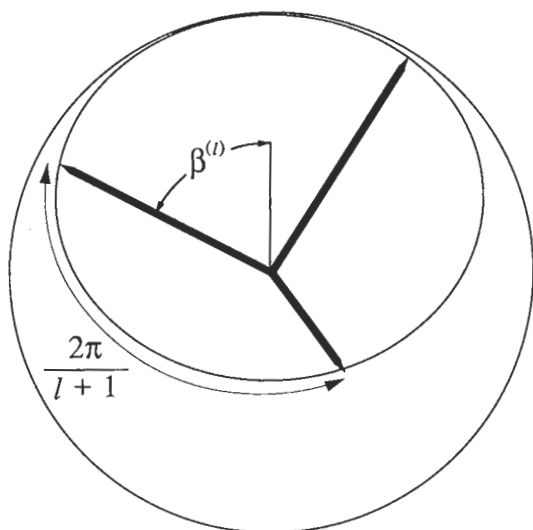


Fig. 3.2 A basic succession of orientations yielding field directions that eliminates anisotropy due to a tensor of rank l . The magnetic field scans $l+1$ directions, forming a cone with apex angle $2\beta^{(l)}$.

with a sampling period of T , followed by a Fourier transformation, gives the average frequency of the transition over the interval. The simplest anisotropic term in the expansion of ω , the dipolar term ω_1 , can be eliminated by summation over two opposite directions, Ω_1^{SFC} and Ω_2^{SFC} , to give a net phase of zero at the sampling point. More generally, the anisotropy described by tensor components $A_{lm \neq 0}$ for a particular l can be averaged away by reorienting the sample so that the field is directed at $N=l+1$ or more directions to form a cone (Fig. 3.2), that is,

$$\Omega_k^{\text{SFC}} \equiv (\alpha_k = \alpha_0 + \frac{2\pi}{N} k, \beta, \gamma), \quad (3.5)$$

because

$$\sum_{k=1}^N D_{m0}^{(l)}(\Omega_k^{\text{SFC}}) = N d_{m0}^{(l)}(\beta) \delta_{m0} \quad (3.6)$$

in eqn (3.4). The remaining term, proportional to A_{l0} , then can be eliminated by a suitable choice of the apex angle $2\beta^{(l)}$:

$$d_{00}^{(l)}(\beta^{(l)}) \equiv P_l(\cos \beta^{(l)}) = 0. \quad (3.7)$$

Values of $\beta^{(l)}$ for tensors up to rank $l=10$ are given in Table 3.1. In real space this approach of discrete orientations has been demonstrated in experiments involving the averaging of chemical shift anisotropy $l=2$ [8]. In this work, the sample was mounted on a goniometer and reoriented so that the magnetic field (in the SFC system) assumed three orthogonal directions during the experiment. As the reorientation process was relatively slow, the magnetization was stored along the field direction during the reorientation. Magic angle spinning can be regarded as a continuous version of this (cubic) symmetry, in which the magnetic field traces out the continuous circle on the sphere, with the apex angle of the underlying cone determined by eqn (3.7).

Table 3.1 Roots of Legendre polynomials of $\cos(\beta^{(l)})$

l	$\beta^{(l)}$				
1	90.00				
2	54.74				
3	39.23	90.00			
4	30.56	70.12			
5	25.02	57.42	90.00		
6	21.18	48.61	76.19		
7	18.36	42.14	66.06	90.00	
8	16.20	37.19	58.30	79.43	
9	14.50	33.28	52.17	71.08	90.00
10	13.12	30.11	47.20	64.32	81.44

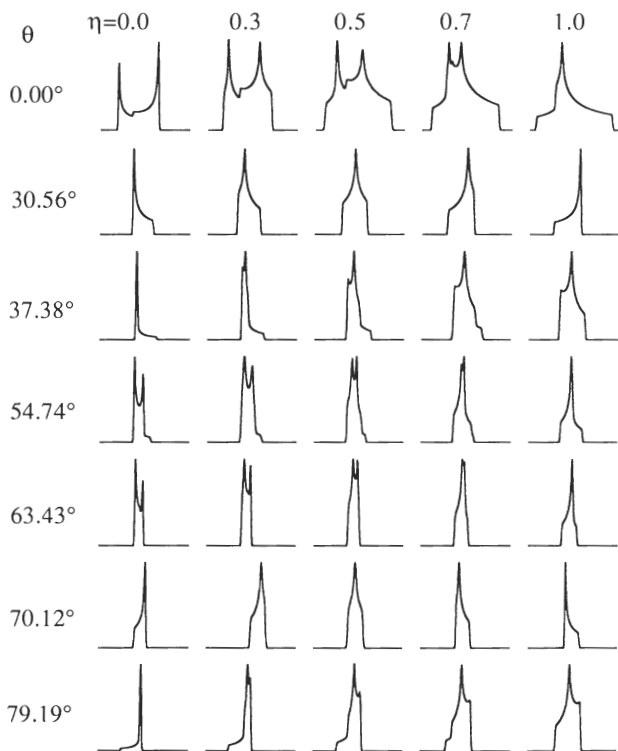


Fig. 3.3 Calculated second-order powder patterns for the central transition of a spin $-\frac{3}{2}$ after motional averaging with a single rotation axis at various angles. 0° (icosahedral angle), 30.56° (root of $P_4(\cos \beta^{(4)})$), 37.38° (icosahedral angle), 54.74° (root of $P_2(\cos \beta^{(2)})$), 63.43° (icosahedral angle), 70.12° (root of $P_4(\cos \beta^{(4)})$), 79.19° (icosahedral angle).

Frequently, however, anisotropic interactions are determined by more than a single rank tensor. Under these conditions the line broadening caused by combining several tensors simultaneously cannot be suppressed by rotation about a single axis, but rather only scaled and altered. For example, the line shape of the central transition for half integer spin quadrupole nucleus is determined by the second- and fourth-rank tensors that describe the second-order effect of the quadrupolar interaction. Figure 3.3 shows various calculated powder patterns of the central transition for spin ($I = \frac{3}{2}$) in a sample spinning around a single axis at different angles. Figure 3.4 shows an experimental example for the ^{23}Na central transition in polycrystalline sodium oxalate at 105.8 MHz. For standard MAS, the powder pattern is determined by the fourth rank tensor (Fig. 3.4(c)). Spinning at either one of the magic angles of the fourth-rank tensor results in spectra with line shapes characteristic of the second-rank tensor (Figs 3.4(b) and (d)), while other possibilities give mixed results with some variation

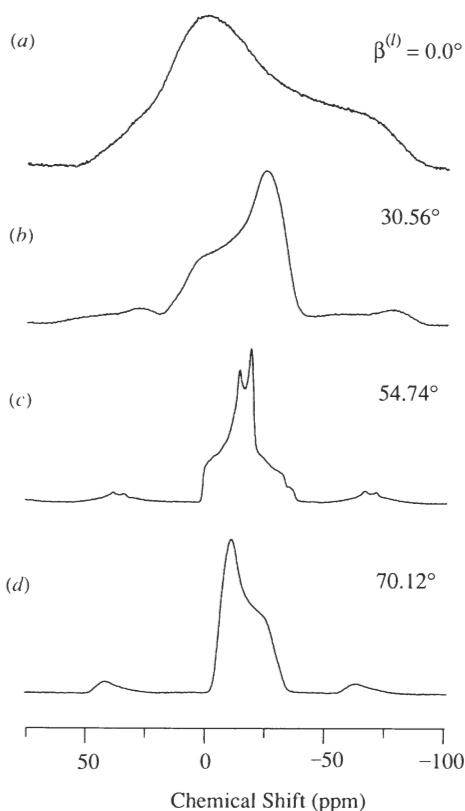


Fig. 3.4 NMR spectrum of the central transition of ^{23}Na in sodium oxalate at 105.8 MHz. (a) Static sample. (b) Sample spinning around axis at 30.56° . (c) Sample spinning around axis at 54.74° . (d) Sample spinning around axis at 70.12° [21].

in linewidth (Fig. 3.3) [9]. It is clear that the anisotropy due to more than one tensorial rank demands a better approximation to spherical symmetry. As an initial possibility we consider point subgroups Γ of $\text{SO}(3)$.

Owing to the high symmetries involved, the effect on the spectral components (eqn 3.1) can be conveniently analysed with group theory. We are interested in the average value of each frequency component over all N symmetry operations G of the group Γ :

$$\bar{\omega}_l^\Gamma = \sum_m A_{lm} \overline{D_{m0}^{(l)}}, \quad (3.8)$$

where

$$\overline{D_{m0}^{(l)}} = \frac{1}{N} \sum_{G \in \Gamma} D_{m0}^{(l)}(\Omega_G). \quad (3.9)$$

The representations of the group $SO(3)$ reduce under subgroup Γ as

$$D_{mn}^{(l)}(\Omega_G) = \sum_{\lambda} a^{(l,\lambda)} D_{mn}^{(l)}(\Omega_G), \quad (3.10)$$

where λ labels the irreducible representation of Γ . The average of the transformation matrices (3.9) and also the averaged frequencies $\bar{\omega}_l^\Gamma$ can be different from zero only if expansion (3.10) contains the totally symmetric representation A_1 of Γ . This follows directly from general orthogonality properties with respect to summation over group elements [10], namely from orthogonality with the symmetric identity representation, while

$$D_{mn}^{(A_1)}(G) = \delta_{mn}. \quad (3.11)$$

The multiplicity $a^{(l,\lambda)}$ of any irreducible representation λ can be evaluated from the general expression for traces

$$a^{(l,\lambda)} = \frac{1}{N} \sum_G \chi^{(l)}(G) \chi^{(\lambda)}(G) \quad (3.12)$$

and the characters calculated from

$$\chi_{(l)}(G) = \sum_m D_{mm}^{(l)}(\Omega_G) = \frac{\sin(l + \frac{1}{2}) \zeta_G}{\sin \frac{1}{2} \zeta_G}, \quad (3.13)$$

where ζ_G is an angle of rotation of the corresponding symmetry operation, related to Euler angles by

$$\zeta_G = 2 \cos^{-1} \left(\cos \frac{\beta_G}{2} \cos \frac{(\alpha_G + \gamma_G)}{2} \right). \quad (3.14)$$

In Table 3.2 are shown characters of reducible $D_{mn}^{(l)}$ for all physically different symmetry operations (classes) of the most symmetrical, icosahedral finite rotation group $\Gamma = I$. In the last column we give the multiplicity of the symmetric representation A_1 after reduction of the original representation $D_{mn}^{(l)}$. Of the first ten anisotropic spectral components, only two ($l=6$ and $l=10$) survive averaging under icosahedral symmetry. A summary of the averaging of tensor components under subgroups of $SO(3)$ is shown in Fig. 3.5. Although icosahedral symmetry is very powerful, it has not yet found any widespread use in NMR except as a special case of dynamic angle spinning (DAS), a point to which we return later.

Selective averaging of interactions with different ranks can be constructed iteratively [11,12]. Given a certain set of directions Ω_k' of the magnetic field in the sample-fixed coordinate (SFC) system, an additional splitting of directions

Table 3.2 Characters of $D^{(l)}$ in the icosahedral subgroup

G	E	$12C_5$	$12C_5^2$	$20C_3$	$15C_2$	
ζ_G	0	72	144	120	180	
l						a^{A_1}
0	1	1	1	1	1	1
1	3	r	\bar{r}	0	-1	0
2	5	0	0	-1	1	0
3	7	$-r$	$-\bar{r}$	1	-1	0
4	9	-1	-1	0	1	0
5	11	1	1	-1	-1	0
6	13	r	\bar{r}	1	1	1
7	15	0	0	0	-1	0
8	17	$-r$	$-\bar{r}$	-1	1	0
9	19	-1	-1	1	-1	0
10	21	1	1	0	1	1

$$r = \frac{1 + \sqrt{5}}{2}, \quad \bar{r} = \frac{1 - \sqrt{5}}{2}$$

around the original ones, as shown in Fig. 3.6, will give a stroboscopic phase of

$$\phi_l(T) = \frac{T}{N'N''} \sum_{mn}^{N'} A_{lm} \sum_k^{N''} D_{mn}^{(l)}(\Omega_k') \sum_j D_{n0}^{(l)}(\Omega_j''). \tag{3.15}$$

After averaging over the first set, Ω_k' , this can be expanded as

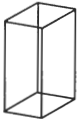
$$\begin{aligned} \phi_l(T) = & \frac{T}{N''} \sum_{n=-l}^l \left(A_{l0} d_{0n}^{(l)}(\beta') d_{n0}^{(l)}(\beta'') \sum_j^{N''} e^{-in(\gamma' + \alpha_j'')} \right. \\ & + \frac{1}{N'} \sum_{m=N'}^l A_{lm} \sum_k^{N'} D_{mn}^{(l)}(\Omega_k') \sum_j^{N''} D_{n0}^{(l)}(\Omega_j'') \\ & \left. + \frac{1}{N'} \sum_{m=-l}^{-N'} A_{lm} \sum_k^{N'} D_{mn}^{(l)}(\Omega_k') \sum_j^{N''} D_{n0}^{(l)}(\Omega_j'') \right), \tag{3.16} \end{aligned}$$

where the last two sums disappear if the multiplicity of the first splitting is $N' > l$.

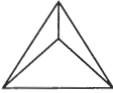
A tensor of any rank l thus can be averaged if either β' or $\beta'' = \beta^{(l)}$, and if the multiplicity of both splittings exceeds the rank, $N', '' > l$. Two possibilities for selecting β allow for simultaneous averaging of two tensors of different ranks. As can be seen from eqn (3.16), the multiplicity of the first splitting can be reduced to $l_1 + 1$ if l_1 is the lowest of the two ranks. In that case the ordering of the apex angles also becomes important: $\beta'' = \beta^{(l_2)}$, otherwise terms $A_{lm} D_{m0}^{(l_2)}(\beta^{(l_2)}) D_{00}^{(l_2)}(\beta^{(l_1)})$, where $m = -l_2, -l_2 + 1, \dots, -N', N', \dots, l_2$ will not be averaged. Extension of this iterative procedure to further terms of different rank is obvious.

Symmetry

$$\langle A_{lm} \rangle = 0$$

**Tetragonal (D_4)**

$$l = \boxed{0} \boxed{1} \boxed{2} \boxed{3} \boxed{4} \boxed{5} \boxed{6} \boxed{7} \boxed{8} \boxed{9} \boxed{10}$$

**Tetrahedral (T)**

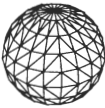
$$l = \boxed{0} \boxed{1} \boxed{2} \boxed{3} \boxed{4} \boxed{5} \boxed{6} \boxed{7} \boxed{8} \boxed{9} \boxed{10}$$

**Octahedral (O)**

$$l = \boxed{0} \boxed{1} \boxed{2} \boxed{3} \boxed{4} \boxed{5} \boxed{6} \boxed{7} \boxed{8} \boxed{9} \boxed{10}$$

**Icosahedral (I)**

$$l = \boxed{0} \boxed{1} \boxed{2} \boxed{3} \boxed{4} \boxed{5} \boxed{6} \boxed{7} \boxed{8} \boxed{9} \boxed{10}$$

**Rotation (SO(3))**

$$l = \boxed{0} \boxed{1} \boxed{2} \boxed{3} \boxed{4} \boxed{5} \boxed{6} \boxed{7} \boxed{8} \boxed{9} \boxed{10}$$

Fig. 3.5 Averaging of spherical harmonics under subgroups of SO(3).

Straightforward extension of the multiple splitting to a continuous trajectory, involving multiple rotations, would also require multiple time dimensions. The ambiguity of the phase parameters γ' in eqn (3.15) however, offers possibilities for a one-dimensional trajectory. Introducing a time dependence

$$\begin{aligned} \gamma_i' + \alpha_j'' &= \gamma_0 + \omega_r t \\ \alpha_i' &= N\omega_r t, \end{aligned} \quad (3.17)$$

we can replace eqn (3.15) by its continuous counterpart

$$\phi_{l_1, l_2}(T) = \sum_{l=l_1, l_2} \sum_{m, n} A_{lm} d_{mn}^{(l)}(\beta^{(l_1)}) d_{n0}^{(l)}(\beta^{(l_2)}) \int_0^T e^{-i\omega_r t(mN+n) + in\gamma_0} dt. \quad (3.18)$$

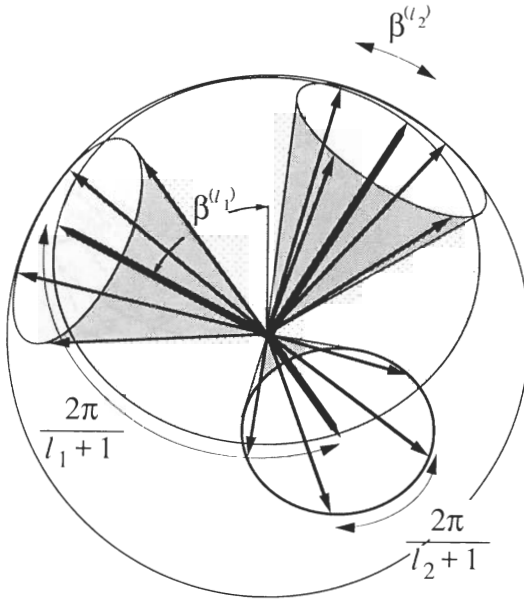


Fig. 3.6 Tensor interactions of two ranks, l_1 and l_2 , can be eliminated with an additional, or secondary splitting, of the field directions under which the interactions are averaged. The symmetry axes of the new cones retain the original symmetry of the primary splitting.

If

$$\omega_r T(mN + n) = k2\pi, \quad k = 1, 2, \dots, \quad (3.19)$$

then expression (3.18) reduces to

$$\phi_{l_1, l_2}(T) = T \sum_l A_{l0} d_{00}^{(l)}(\beta^{(l_1)}) d_{00}^{(l)}(\beta^{(l_2)}) = 0, \quad (3.20)$$

which describes a rotation of the field direction (in the SFC system) with a continuous change in the rotation axis (Fig. 3.7). Vertices of polygons with apex angle $2\beta^{(l_2)}$ exactly fit this trajectory, while the symmetry axes of the polygons trace out a cone with apex angle $2\beta^{(l_1)}$.

The iterative geometry described above was first applied to the averaging of second and third rank interactions in spin space, using double modulation of the CW irradiation [13]. In real space, applications based on an iterative scheme were used to average second-order quadrupole line broadening [14]. The fast reorientation is performed with a double rotor assembly (DOR), in which a powder sample is placed in a small rotor, spinning inside a larger rotor [15,16]. The spinning axis is inclined at the angle $\beta^{(4)}$ relative to the symmetry axis of

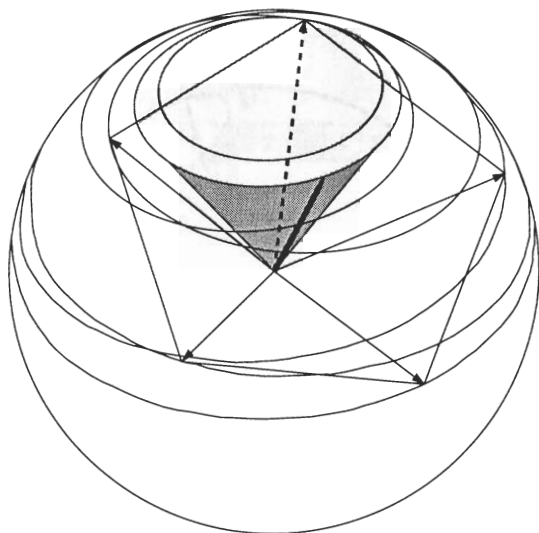


Fig. 3.7 A continuous one-dimensional trajectory to eliminate two tensors. A complementary set of points (commensurate with the basic splitting) can be found at every point on the trajectory, to average one of the tensors. Such a set is shown here as a pentagon. The centres of the pentagons form a continuous cone with apex angle such that another tensor will be averaged.

the outer rotor, which is itself spinning at $\beta^{(2)}$ relative to the magnetic field direction.

The third (and probably most general) averaging scheme, dubbed dynamic angle spinning (DAS) [17,18], is suggested by the patterns in Fig. 3.4. Note that two of the line shapes (Figs 3.4(b) and (d)) are in fact mirror images with different scaling factors. The reflection symmetry about an isotropic shift value is caused by a sign inversion of $P_2(\cos \beta^{(4)})$, and the scaling ratio is given by

$$\left| \frac{P_2(\cos \beta_1^{(4)})}{P_2(\cos \beta_2^{(4)})} \right| = 1.87, \quad (3.21)$$

where $\beta_1^{(4)} = 30.56^\circ$ and $\beta_2^{(4)} = 70.12^\circ$, respectively. Since the shift reflection occurs with the same scaling ratio for each particle in the sample, it is possible to re-phase the signal of all particles simultaneously at some time T . If evolution for a period τT proceeds at the angle β_1 , and subsequently for a period $(1 - \tau)T$ at β_2 , the accumulated anisotropic phase will be

$$\phi(T) = \int_0^T \omega(\beta(t)) dt = (\omega(\beta_1)\tau + \omega(\beta_2)(1 - \tau))T. \quad (3.22)$$

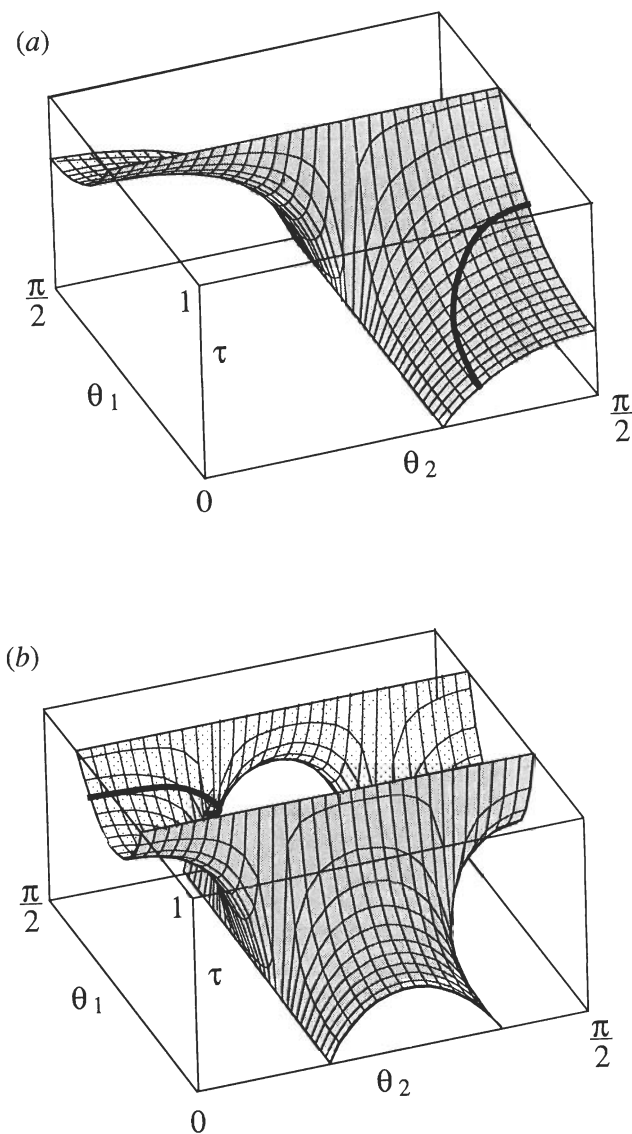


Fig. 3.8 Solution of equation (3.23) for refocusing of tensor interactions of (a) second rank and (b) fourth rank, in a polycrystalline sample. The line of intersection of the two surfaces, shown as a bold line, gives the simultaneous solution for anisotropies of both ranks. The bold lines are related to the curves of θ_1 and θ_2 versus τ in Fig. 3 of [18].

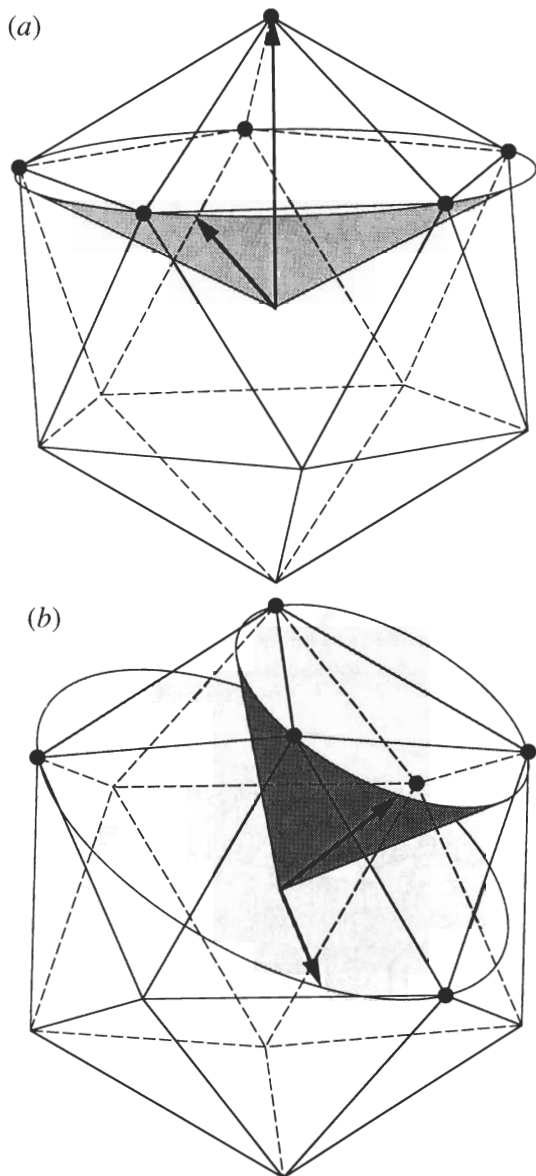


Fig. 3.9 Icosahedral symmetry can be implemented with just two continuous trajectories in cases where tensors of rank 2 and 4 are to be eliminated. In the laboratory frame, this appears as a fast rotation of the sample at two different angles in succession. Time spent along one particular trajectory is proportional to the number of vertices. In (a) the vertices are those of an icosahedron, the two spinning axes are $\beta_1^{(l)} = 0^\circ$ and $\beta_2^{(l)} = 63.43^\circ$, and the ratio of times spinning at the two angles is 1:5. In (b) the vertices are those of either an icosahedron or a dodecahedron, the angles are $\beta_1^{(l)} = 37.38^\circ$ and $\beta_2^{(l)} = 79.12^\circ$, and the ratio of times spinning at the two angles is 1:1.

The modulation (3.22) disappears for each interaction of rank l if

$$P_l(\cos \beta_1) \tau + P_l(\cos \beta_2) (1 - \tau) = 0, \quad (3.23)$$

which results in $\phi(T) = 0$. A signal recorded at constant intervals of time $T, 2T, 3T, \dots$ then will be independent of all anisotropic terms, and carry information only about the available isotropic shifts.

Many variations of this approach are possible because motion of the spinning axis is not limited to discrete positions and equal probability. Any function of time $\beta(t)$, satisfying the condition

$$\int_0^T \omega(\beta(t)) p(t) dt = 0 \quad (3.24)$$

where $p(t)$ is a weight function, will periodically refocus the phase. For example, a linear sweep of the spinning axis between the angles 19.05° and 99.19° is a solution to eqn (3.24). Similarly, the above DOR trajectory can be understood as

$$\cos \beta(t) = \cos \beta^{(2)} \cos \beta^{(4)} + \sin \beta^{(2)} \sin \beta^{(4)} \cos \omega_r t \quad (3.25)$$

and $p(t) = 1$, where ω_r is the spinning speed of the outer spinner, and $\beta^{(2)}$ and $\beta^{(4)}$ are the magic angles of the Legendre polynomials $P_2(\cos \beta)$ and $P_4(\cos \beta)$. The DAS trajectories can also follow the symmetry of regular polyhedra. The solutions of eqn (3.23) generally describe surfaces in three-dimensional space (β_1, β_2, τ) , as shown in Fig. 3.8. Since the spinning angles can be interchanged, the surfaces exhibit inversion symmetry. A simultaneous solution for two equations of the form (3.23) is obtained at any point on a crossing line of two surfaces (Fig. 3.6). Two solutions, $(37.38^\circ, 79.19^\circ, \frac{1}{2})$ and $(0^\circ, 63.43^\circ, \frac{1}{6})$, describe circles which traverse the vertices of an icosahedron (Fig. 3.9) and thus present continuous extensions of icosahedral point symmetry. One of the solutions may be converted to the other just by inversion of one direction. Equation (3.22) also can be extended to give solutions for averaging three and more tensors, with the addition of controlled time delays and spinning angles. Such experiments will be successful if the motion of the spinning axis is fast compared to the transverse relaxation rate, or if the transient magnetization can be stored along the polarizing field. The latter method was actually used in dynamic angle spinning (DAS) experiments to remove second-order quadrupole line broadening in spectra of ^{17}O [19]. We close by mentioning that averaging by icosahedral symmetry (or double rotation) in both spin and space coordinates simultaneously is an optimal solution for zero-field NMR in high field [20]. Mueller has discussed these new averaging techniques in detail, and his thesis [21] contains a number of applications.

Acknowledgements

We are grateful to Michael Munowitz and Karl Mueller for their invaluable comments and assistance. This work was supported by the Director, Office of Energy Research, Office of Basic Energy Sciences, Materials Sciences Division of the U.S. Department of Energy under Contract No. DE-AC03-76SF00098.

References

1. Hahn, E. L. (1950). *Phys. Rev.*, **80**, 580.
2. Carr, H. Y. and Purcell, E. M. (1954). *Phys. Rev.*, **94**, 630.
3. Anderson, W. A. and Arnold, J. T. (1954). *Phys. Rev.*, **94**, 497.
4. Waugh, J. S., Huber, L. M., and Haeberlen, U. (1968). *Phys. Rev. Lett.*, **20**, 180.
5. Andrew, E. R., Bradbury, A., and Eades, R. G. (1958). *Nature*, **182**, 1659.
6. Lowe, I. J. (1959). *Phys. Rev. Lett.*, **2**, 285.
7. Zwanziger, J. W., Koenig, M., and Pines, A. (1990). *Ann. Rev. Phys. Chem.*, **41**, 601.
8. Bax, A., Szeverenyi, N. M., and Maciel, G. (1983). *J. Magn. Reson.*, **52**, 147.
9. Ganapathy, S., Schramm, S., and Oldfield, E. (1982). *J. Chem. Phys.*, **77**, 4360.
10. Hamermesh, M. (1962) *Group theory and its application to physical problems*. Addison Wesley, London (rpt. Dover, New York, 1989).
11. McLaren, A. D. (1963). *Math. Comput.*, **17**, 361.
12. Konyaev, S. I. (1979). *Mathematical Notes of the Acad. Sci. USSR*, **25**, 629 (p. 326 Engl. tr.).
13. Mefed, A. E. (1984). *Sov. J. Exp. Theor. Phys.*, **86**, 302.
14. Samoson, A., Lippmaa, E., and Pines, A. (1988). *Mol. Phys.*, **65**, 1013.
15. Samoson, A., and Pines, A. (1989). *Rev. Sci. Instrum.*, **60**, 3239.
16. Wu, Y., Sun, B. Q., Pines, A., Samoson, A., and Lippmaa, E. (1990). *J. Magn. Reson.*, **89**, 297.
17. Llor, A., and Virlet, J. (1988). *Chem. Phys. Lett.*, **152**, 248.
18. Mueller, K. T., Sun, B.-Q., Chingas, G. C., Zwanziger, J. W., Terao, T., and Pines, A. (1990). *J. Magn. Reson.*, **86**, 470.
19. Chmelka, B. F., Mueller, K. T., Pines, A., Stebbins, J., Wu, Y., and Zwanziger, J. W. (1989). *Nature*, **339**, 42.
20. Tycko, R. (1988). *Phys. Rev. Lett.*, **60**, 2734.
21. Mueller, K. T. (1991). *Ph.D. thesis*. University of California, Berkeley.